Control of Magnetic Space Tug

Emilien Fabacher * **Daniel Alazard** * **Finn Ankersen** **
Stéphanie Lizy-Destrez * **Léonore de Mijolla** ***

* *ISAE-SUPAERO, Toulouse, France (emilien.fabacher@isae.fr).*
** *ESTEC, Noordwijk, The Netherlands*
*** *Airbus DS, Les Mureaux, France*

Abstract: Magnetic tugging of a target satellite without thrust capacity can be interesting in various contexts. In this paper, the dynamics of such a 2-satellites formation is derived and linearised about a nominal configuration which is not necessarily constant. Analytical expressions are given for the different forces and torques differentials. Two LQ-based controllers are given, depending on the capacity of the target to control its own attitude. Linear simulations of the closed loop system are realised and compared with the full order non-linear model. The results obtained are promising and consistent with previous research.

Keywords: Formation flying; Spacecraft dynamics, navigation, guidance and control

1. INTRODUCTION

Satellite tugging can be motivated by various reasons: de-orbiting or re-orbiting, necessary in the case of satellites end-of-life; orbit control for formations of several satellites in which only one is equipped with thrusters; or to finalize launches, in which case this manoeuvre would replace the last stage of the launcher.

Several means can be considered to modify the orbit of a satellite by tugging it with another satellite. Indeed, one could simply dock a chaser/tug satellite to the target/tugged satellite. Contactless solutions however could be more interesting, as they could provide a way to avoid standardized interfaces and hazardous docking phases. They may also help preventing the creation of new debris.

In the same context as Voirin et al. (2012), we propose using magnetic forces to tug the target. Indeed many satellites, especially in Low Earth Orbit, are equipped with Magnetic Torque Bars (MTQs), used for attitude control. A chaser equipped with a powerful magnetic dipole could generate forces and torques on the target.

Electromagnetic Formation Flying has been studied since the beginning of the 21$^{\text{st}}$ century. Schweighart (2005) computed the dipoles to apply to make a N-satellites formation follow a given trajectory in free space; Elias et al. (2007) gave a way to control the relative position of a formation, while controlling each satellite attitude with reaction wheels; Sakai et al. (2008) solved the guidance to keep the same position in time and suggested to modulate the dipole with sine waves to avoid the problem caused by the constant torque due to the Earth magnetic field; Ahsun et al. (2010) improved the work done by Elias et al. (2007) and applied an idea similar to Sakai et al. (2008). Recently, Huang et al. (2016) started looking for configurations enabling to reduce the total momentum on a 2-satellites formation.

All the previously cited references assumed the dipoles to be located at the center of mass of the satellites, and supposed all satellites equally capable of steering their dipole and controlling their attitude. In this study, we consider a lever-arm on the target dipole, and assume both the value and orientation of the target dipole fixed in its body frame. The target attitude will be supposed uncontrolled in some examples. Finally, a constant thrust from the chaser is considered, which changes the dynamics compared to the given references.

In a paper to be published, the authors will demonstrate the existence of nominal relative configuration trajectories enabling to magnetically tug a target satellite, while avoiding accumulating angular momentum because of the Earth magnetic field, without waving the dipoles.

This paper focuses on the control of the formation around these configuration trajectories. The system considered is described in section 2; the equations of motion are derived in section 3; they are linearised in section 4 while the efforts are differentiated in section 5; finally, section 6 presents two possible controllers.

2. SYSTEM DESCRIPTION

The system considered is composed of a target satellite denoted by the subscript T and a chaser satellite subscripted C. As presented in Fig. 1, the target is equipped with an MTQ turned on which dipole is equal to the constant $\boldsymbol{\mu}_T = [0\ 500\ 0]^T$ A m^2 in its body frame (value reached by Sentinel 2 satellite for example [1]), located at the body-frame constant position $\boldsymbol{\gamma}_{\mu_T} = [1\ 0\ 0]^T$ m; the target mass is $\mathbf{m}_T = 2300$ kg; its inertia tensor is $\mathbf{J}_T = \text{diag}\left([1300\ 1100\ 700]\right)$ kg m^2. The chaser is characterised by $\mathbf{m}_C = 1000$ kg; $\mathbf{J}_C = 700\ \mathbf{I}_3$ kg m^2, where $\mathbf{I}_3$ is the identity matrix. Its dipole is located at its center of mass ($\boldsymbol{\gamma}_{\mu_C} = \mathbf{0}$).

[1] http://emits.sso.esa.int/emits-doc/ESTEC/Sentinel-1-FP7-Industry-Day-Nov-07.pdf
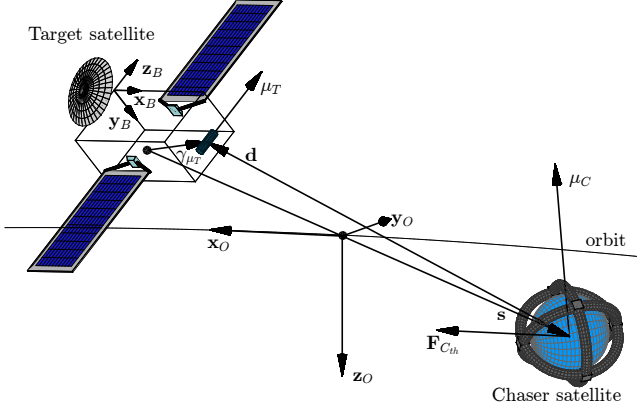
Fig. 1. Vectors and frames used in this article.

For a given vector $\mathbf{x}$, x is the norm of the vector, $\hat{\mathbf{x}}$ is the unitary vector associated, $\dot{x}$ is its time derivative in the specified reference frame. $[\mathbf{x}^\times]$ is the skew-symmetric matrix denoting the cross-product $\mathbf{x}\times$, $\cdot$ denotes the scalar product. Four frames are used in this article; I, an inertial frame centred on the Earth; O, the orbital frame centred on the center of mass of the formation; B_i, the body frame linked to satellite i (target if no i specified).

3. DYNAMICS

3.1 Relative Position Dynamics

Law describing the evolution of the relative position $\mathbf{s}$ between the target and the chaser has been showed in Fabacher et al. (2015). In inertial frame, this evolution is given by:

$$\left.\frac{d^2\mathbf{s}}{dt^2}\right|_I = -\frac{\mu}{r^3}\mathbf{M}\mathbf{s} + \frac{\mathbf{F}_{C_{th}}}{m_C} - \frac{\mathbf{F}_{T_{\epsilon\mu}}}{m_{CT}} \tag{1}$$

where $\mathbf{M}$ is the Jacobian matrix describing the linearisation of the Earth gravity with regard to the position around the center of mass of the formation, and can be obtained from Wie (1998). μ is the standard gravitational parameter of the Earth; r is the distance between the center of the Earth and the formation's center of mass; $\mathbf{F}_{C_{th}}$ is the force created by the chaser's thrusters; $\mathbf{F}_{T_{\epsilon\mu}}$ is the magnetic force created by the chaser's magnetic dipole on the target's magnetic dipole; m_{CT} is the reduced mass of the system ($m_{CT} = \frac{m_C m_T}{m_C+m_T}$).

Differentiating twice $\mathbf{s}$ in the orbital frame gives (2):

$$\left.\frac{d^2\mathbf{s}}{dt^2}\right|_I = \left.\frac{d^2\mathbf{s}}{dt^2}\right|_O + \boldsymbol{\omega}\times(\boldsymbol{\omega}\times\mathbf{s}) + 2\boldsymbol{\omega}\times\left.\frac{d\mathbf{s}}{dt}\right|_O + \left.\frac{d\boldsymbol{\omega}}{dt}\right|_O\times\mathbf{s} \tag{2}$$

where $\boldsymbol{\omega}$ is the rotational rate vector from inertial to orbital frame. We define $\boldsymbol{\eta} = \frac{d\boldsymbol{\omega}}{dt}$ which, as $\boldsymbol{\omega}$, depends on the position of the formation in its orbit. The equation of the relative motion in the orbital frame is therefore:

$$\ddot{\mathbf{s}} + \boldsymbol{\omega}\times(\boldsymbol{\omega}\times\mathbf{s}) + 2\boldsymbol{\omega}\times\dot{\mathbf{s}} + \boldsymbol{\eta}\times\mathbf{s} + \frac{\mu}{r^3}\mathbf{M}\mathbf{s} = \frac{\mathbf{F}_{C_{th}}}{m_C} - \frac{\mathbf{F}_{T_{\epsilon\mu}}}{m_{CT}} \tag{3}$$

3.2 Attitude Dynamics

In the body frame, the evolution of the attitude of one of the satellites is classically described by:

$$\mathbf{J}\frac{d\boldsymbol{\omega}_{B/I}}{dt} + \boldsymbol{\omega}_{B/I}\times\mathbf{J}\boldsymbol{\omega}_{B/I} = \sum\boldsymbol{\tau} \tag{4}$$

In the case of Electromagnetic Formation Flight, $\sum\boldsymbol{\tau}$ can be developed in:

$$\sum\boldsymbol{\tau} = \boldsymbol{\tau}_{\epsilon\mu} + \boldsymbol{\tau}_\gamma + \boldsymbol{\tau}_{\epsilon\mu E} + \boldsymbol{\tau}_{rw} + \boldsymbol{\tau}_g + \boldsymbol{\tau}_p \tag{5}$$

with $\boldsymbol{\tau}_{\epsilon\mu}$ the torque on the satellite due to the magnetic field created by the other satellite; $\boldsymbol{\tau}_\gamma = \boldsymbol{\gamma}_{\mu_T}\times\mathbf{F}_{\epsilon\mu}$ the torque created by the cross product of the satellite center of mass to dipole lever-arm with the magnetic force created by the other satellite; $\boldsymbol{\tau}_{\epsilon\mu E}$ the torque on the satellite due to the Earth magnetic field; $\boldsymbol{\tau}_{rw}$ the torque created by a reaction wheel system (or other similar devices); $\boldsymbol{\tau}_g$ the torque due to the gravity gradient; $\boldsymbol{\tau}_p$ the rest of the perturbing torques.

3.3 Nominal States

The guidance of the formation is developed in Fabacher et al. (2015) and will be further studied in a future reference. Because r, $\boldsymbol{\omega}$, $\boldsymbol{\eta}$ and the Earth magnetic field vary in orbit, the nominal parameters states also depend on the time. They solve the system of differential equation formed by (3), (4) adapted for the chaser and (4) adapted for the target. In the scope of this article, we will consider that for every time t, a nominal configuration trajectory has been found and is described by a combination $\left(\mathbf{s}, \dot{\mathbf{s}}, \boldsymbol{\theta}_C, \boldsymbol{\omega}_{B/O_C}, \boldsymbol{\theta}_T, \boldsymbol{\omega}_{B/O_T}, \mathbf{F}_{C_{th}}, \boldsymbol{\tau}_{C_{rw}}, \boldsymbol{\mu}_C, \boldsymbol{\tau}_{T_{rw}}\right)_{nom}(t)$.

4. LINEARISATION: DYNAMICS AND KINEMATICS

In this section, the dynamics equations are differentiated around a nominal trajectory. The aim is to obtain a time-varying state space system representation which will be used to synthesize controllers.

4.1 Translational Motion

Let's differentiate (3):

$$\ddot{\boldsymbol{\delta}}\mathbf{s} + 2\left[\boldsymbol{\omega}^\times\right]\dot{\boldsymbol{\delta}}\mathbf{s} + \left(\left[\boldsymbol{\omega}^\times\right]^2 + \left[\boldsymbol{\eta}^\times\right] + \frac{\mu}{r^3}\mathbf{M}\right)\boldsymbol{\delta}\mathbf{s}$$
$$= \frac{\boldsymbol{\delta}\mathbf{F}_{C_{th}}}{m_C} - \frac{\boldsymbol{\delta}\mathbf{F}_{T_{\epsilon\mu}}}{m_{CT}} \tag{6}$$

$\boldsymbol{\delta}\mathbf{F}_{T_{\epsilon\mu}}$ is the differentiation of the magnetic force considered in the problem. Part of it comes from the relative position, the rest comes from the control inputs $\boldsymbol{\delta}\boldsymbol{\mu}_C$.

$$\boldsymbol{\delta}\mathbf{F}_{T_{\epsilon\mu}} = \frac{\partial\mathbf{F}_{T_{\epsilon\mu}}}{\partial\mathbf{s}}\boldsymbol{\delta}\mathbf{s} + \frac{\partial\mathbf{F}_{T_{\epsilon\mu}}}{\partial\boldsymbol{\mu}_C}\boldsymbol{\delta}\boldsymbol{\mu}_C \tag{7}$$

Similarly, $\boldsymbol{\delta}\mathbf{F}_{C_{th}}$ is the differentiation of the thruster force considered in the problem. It is considered as a control input. The previous equation can be derived in a state space representation as follows:

$$\begin{bmatrix}\dot{\boldsymbol{\delta}}\mathbf{s} \\ \ddot{\boldsymbol{\delta}}\mathbf{s}\end{bmatrix} = \mathbf{A}_s\begin{bmatrix}\boldsymbol{\delta}\mathbf{s} \\ \dot{\boldsymbol{\delta}}\mathbf{s}\end{bmatrix} + \mathbf{B}_s\begin{bmatrix}\boldsymbol{\delta}\mathbf{F}_{C_{th}} \\ \boldsymbol{\delta}\boldsymbol{\mu}_C\end{bmatrix} \tag{8}$$

With:

$$\mathbf{A}_s = \begin{bmatrix}\mathbf{0}_3 & \mathbf{I}_3 \\ -\left(\left[\boldsymbol{\omega}^\times\right]^2 + \left[\boldsymbol{\eta}^\times\right] + \frac{\mu}{r^3}\mathbf{M}\right) & -2\left[\boldsymbol{\omega}^\times\right]\end{bmatrix}$$
$$+ \begin{bmatrix}\mathbf{0}_3 & \mathbf{0}_3 \\ -\frac{1}{m_{CT}}\frac{\partial\mathbf{F}_{T_{\epsilon\mu}}}{\partial\mathbf{s}} & \mathbf{0}_3\end{bmatrix} \tag{9}$$

and

$$\mathbf{B}_s = \begin{bmatrix}\mathbf{0}_3 & \mathbf{0}_3 \\ \frac{1}{m_C}\mathbf{I}_3 & \frac{-1}{m_{CT}}\frac{\partial\mathbf{F}_{T_{\epsilon\mu}}}{\partial\boldsymbol{\mu}_C}\end{bmatrix} \tag{10}$$

4.2 Attitude Motion

For each satellite, the motion is linearised around $\dot{\boldsymbol{\omega}}_{B/I_{nom}}$, $\boldsymbol{\omega}_{B/I_{nom}}$ and the attitude in the orbital frame represented by $\boldsymbol{\theta}_{nom}$. Linearising (4) and restricting to first order terms then yields:

$$\mathbf{J}\dot{\boldsymbol{\delta\omega}}_{B/I} + \left(\left[\boldsymbol{\omega}_{B/I_{nom}}{}^{\times}\right]\mathbf{J} - \left[\mathbf{J}\boldsymbol{\omega}_{B/I_{nom}}{}^{\times}\right]\right)\boldsymbol{\delta\omega}_{B/I} = \sum \boldsymbol{\delta\tau} \tag{11}$$

As

$$\boldsymbol{\omega}_{B/I} = \boldsymbol{\omega}_{B/O} + \boldsymbol{\omega}_{O/I} = \boldsymbol{\omega}_{B/O} - \omega\hat{\mathbf{y}}_O \tag{12}$$

the rotation rate vector is given in the body frame by Wie (1998):

$$\boldsymbol{\omega}_{B/I_B} = \mathbf{C}_2\dot{\boldsymbol{\theta}} - \omega\mathbf{P}_{O\to B}\begin{bmatrix}0 & 1 & 0\end{bmatrix}^T \tag{13}$$

with (using the 321 Euler angles convention):

$$\mathbf{C}_2 = \begin{bmatrix} 1 & 0 & -\sin\theta_2 \\ 0 & \cos\theta_1 & \sin\theta_1\cos\theta_2 \\ 0 & -\sin\theta_1 & \cos\theta_1\cos\theta_2 \end{bmatrix} \tag{14}$$

As $\boldsymbol{\omega}_{B/O} = \mathbf{C}_2\dot{\boldsymbol{\theta}}$, linearising (13) yields:

$$\boldsymbol{\delta\omega}_{B/I_B} = (\mathbf{C}_3 - \omega\mathbf{C}_1)\boldsymbol{\delta\theta} + \mathbf{C}_2\dot{\boldsymbol{\delta\theta}} \tag{15}$$

where, with $s_i = \sin\theta_i$ and $c_i = \cos\theta_i$, $\mathbf{C}_1$ and $\mathbf{C}_3$ are defined by:

$$\mathbf{C}_1 = \begin{bmatrix} 0 & -s_2s_3 & c_2c_3 \\ c_1s_2s_3 - c_3s_1 & c_2s_1s_3 & c_3s_1s_2 - c_1s_3 \\ -c_1c_3 - s_1s_2s_3 & c_1c_2s_3 & s_1s_3 + c_1c_3s_2 \end{bmatrix} \tag{16}$$

$$\mathbf{C}_3 = \begin{bmatrix} \dfrac{\partial\mathbf{C}_2}{\partial\theta_1}\dot{\boldsymbol{\theta}} & \bigg| & \dfrac{\partial\mathbf{C}_2}{\partial\theta_2}\dot{\boldsymbol{\theta}} & \bigg| & \dfrac{\partial\mathbf{C}_2}{\partial\theta_3}\dot{\boldsymbol{\theta}} \end{bmatrix} \tag{17}$$

We then have:

$$\dot{\boldsymbol{\delta\theta}} = \mathbf{C}_2^{-1}(\omega\mathbf{C}_1 - \mathbf{C}_3)\boldsymbol{\delta\theta} + \mathbf{C}_2^{-1}\boldsymbol{\delta\omega}_{B/I} \tag{18}$$

The state space representation of the linearised attitude dynamics of satellite i is hence:

$$\begin{bmatrix} \dot{\boldsymbol{\delta\theta}}_i \\ \dot{\boldsymbol{\delta\omega}}_{i_{B/I}} \end{bmatrix} = \mathbf{A}_{i_\theta}\begin{bmatrix} \boldsymbol{\delta\theta}_i \\ \boldsymbol{\delta\omega}_{i_{B/I}} \end{bmatrix} + \mathbf{B}_{i_\theta}\boldsymbol{\delta u}_i \tag{19}$$

With:

$$\mathbf{A}_{i_\theta} = \begin{bmatrix} \mathbf{C}_{2_i}^{-1}(\omega\mathbf{C}_{1_i} - \mathbf{C}_{3_i}) & \mathbf{C}_{2_i}^{-1} \\ \mathbf{J}_i^{-1}\dfrac{\partial\sum\boldsymbol{\delta\tau}_i}{\partial\theta_i} & -\mathbf{J}_i^{-1}\left(\left[\boldsymbol{\omega}_{i_{B/I}}{}^{\times}\right]\mathbf{J}_i - \left[\mathbf{J}_i\boldsymbol{\omega}_{i_{B/I}}{}^{\times}\right]\right) \end{bmatrix} \tag{20}$$

And the matrix $\mathbf{B}_{i_\theta}$ depends on the actuators considered. In the frame of magnetic tugging, we will consider that the actuators used for the control of the attitude are both the magnetic dipole of the chaser $\boldsymbol{\delta\mu}_C$, and a dedicated AOCS (Attitude and Orbit Control System), composed either of reaction wheels or of control momentum gyroscopes for which the torque $\boldsymbol{\delta\tau}_{i_{rw}}$ will be the controlled input:

$$\boldsymbol{\delta u}_i = \begin{bmatrix} \boldsymbol{\delta\tau}_{i_{rw}} \\ \boldsymbol{\delta\mu}_C \end{bmatrix} \tag{21}$$

The expression of the matrix $\mathbf{B}_{i_\theta}$ is then:

$$\mathbf{B}_{i_\theta} = \begin{bmatrix} \mathbf{0}_3 & \mathbf{0}_3 \\ \mathbf{J}_i^{-1} & \mathbf{J}_i^{-1}\dfrac{\partial\boldsymbol{\tau}_{i_{\epsilon\mu}}}{\partial\boldsymbol{\mu}_C} \end{bmatrix} \tag{22}$$

The reference frame is the orbital frame, therefore, the parameters measured are $\boldsymbol{\delta\theta}$ and $\boldsymbol{\omega}_{B/O}$. The measure equation is therefore:

$$\mathbf{y} = \underbrace{\begin{bmatrix} \mathbf{I}_3 & \mathbf{0}_3 \\ \omega\mathbf{C}_{1_i} & \mathbf{I}_3 \end{bmatrix}}_{\mathbf{C}_{i_\theta}}\begin{bmatrix} \boldsymbol{\delta\theta}_i \\ \boldsymbol{\delta\omega}_{i_{B/I}} \end{bmatrix} \tag{23}$$

4.3 Coupled Linear Dynamics

In the previous sections, the evolution of the attitude of both satellites have been linearised, as well as the dynamics of the relative position. However, in this linearisation, the couplings between these three different dynamics have been neglected. In this section, the complete linear model of the formation is therefore developed.

We consider the state vector defined by

$$\mathbf{x} = \begin{bmatrix} \boldsymbol{\delta s} & \dot{\boldsymbol{\delta s}} & \boldsymbol{\delta\theta}_C & \boldsymbol{\delta\omega}_{C_{B/O}} & \boldsymbol{\delta\theta}_T & \boldsymbol{\delta\omega}_{T_{B/O}} \end{bmatrix}^T \tag{24}$$

and the control input

$$\mathbf{u} = \begin{bmatrix} \boldsymbol{\delta F}_{C_{th}} & \boldsymbol{\delta\tau}_{C_{rw}} & \boldsymbol{\delta\mu}_C & \boldsymbol{\delta\tau}_{T_{rw}} \end{bmatrix}^T \tag{25}$$

Then the linearised (time dependent) system $\mathbf{G}(t)$ is:

$$\begin{aligned} \dot{\mathbf{x}} &= \mathbf{A}(t)\mathbf{x} + \mathbf{B}(t)\mathbf{u} \\ \mathbf{y} &= \mathbf{C}(t)\mathbf{x} \end{aligned} \tag{26}$$

$$\mathbf{A}(t, \mathbf{s}(t), \boldsymbol{\theta}_C(t), \boldsymbol{\theta}_T(t), ...) =$$

$$\left[\begin{array}{cc|cc|cc} \multicolumn{2}{c|}{\mathbf{A}_s} & \mathbf{0}_3 & \mathbf{0}_3 & \mathbf{0}_3 & \mathbf{0}_3 \\ & & \frac{-1}{m_{CT}}\frac{\partial\mathbf{F}_{T_{\epsilon\mu}}}{\partial\boldsymbol{\theta}_C} + \frac{1}{m_C}\frac{\partial\mathbf{F}_{C_{th}}}{\partial\boldsymbol{\theta}_C} & \mathbf{0}_3 & \frac{-1}{m_{CT}}\frac{\partial\mathbf{F}_{T_{\epsilon\mu}}}{\partial\boldsymbol{\theta}_T} & \mathbf{0}_3 \\ \hline \mathbf{0}_3 & \mathbf{0}_3 & \multicolumn{2}{c|}{} & \mathbf{0}_3 & \mathbf{0}_3 \\ \mathbf{J}_C^{-1}\frac{\partial\boldsymbol{\tau}_{C_{\epsilon\mu}}}{\partial\mathbf{s}} & \mathbf{0}_3 & \multicolumn{2}{c|}{\mathbf{A}_{C_\theta}} & \mathbf{J}_C^{-1}\frac{\partial\sum\boldsymbol{\tau}_C}{\partial\boldsymbol{\theta}_T} & \mathbf{0}_3 \\ \hline \mathbf{0}_3 & \mathbf{0}_3 & \mathbf{0}_3 & \mathbf{0}_3 & \multicolumn{2}{c}{} \\ \mathbf{J}_T^{-1}\frac{\partial\boldsymbol{\tau}_{T_{\epsilon\mu}}}{\partial\mathbf{s}} & \mathbf{0}_3 & \mathbf{J}_T^{-1}\frac{\partial\sum\boldsymbol{\tau}_T}{\partial\boldsymbol{\theta}_C} & \mathbf{0}_3 & \multicolumn{2}{c}{\mathbf{A}_{T_\theta}} \end{array}\right] \tag{27}$$

$$\mathbf{B}(t, ...) = \begin{bmatrix} \mathbf{0}_3 & \mathbf{0}_3 & \mathbf{0}_3 & \mathbf{0}_3 \\ \frac{1}{m_C}\mathbf{I}_3 & \mathbf{0}_3 & \frac{-1}{m_{CT}}\frac{\partial\mathbf{F}_{T_{\epsilon\mu}}}{\partial\boldsymbol{\mu}_C} & \mathbf{0}_3 \\ \mathbf{0}_3 & \mathbf{0}_3 & \mathbf{0}_3 & \mathbf{0}_3 \\ \mathbf{0}_3 & \mathbf{J}_C^{-1} & \mathbf{J}_C^{-1}\frac{\partial\boldsymbol{\tau}_{C_{\epsilon\mu}}}{\partial\boldsymbol{\mu}_C} & \mathbf{0}_3 \\ \mathbf{0}_3 & \mathbf{0}_3 & \mathbf{0}_3 & \mathbf{0}_3 \\ \mathbf{0}_3 & \mathbf{0}_3 & \mathbf{J}_T^{-1}\frac{\partial\boldsymbol{\tau}_{T_{\epsilon\mu}}}{\partial\boldsymbol{\mu}_C} & \mathbf{J}_T^{-1} \end{bmatrix} \tag{28}$$

$$\mathbf{C}(t, ...) = \begin{bmatrix} \mathbf{I}_6 & & \\ & \mathbf{C}_{C_\theta} & \\ & & \mathbf{C}_{T_\theta} \end{bmatrix} \tag{29}$$

5. LINEARISATION: FORCES AND TORQUES

5.1 Linearised Forces

The two forces $\mathbf{F}_{T_{\epsilon\mu}}$ and $\mathbf{F}_{C_{th}}$ depend on the relative position and orientation of the satellites in the formation. Indeed, the thrust $\mathbf{F}_{C_{th}}$ is created by the chaser relatively to its own body frame, therefore the thrust in the orbital frame evolves with the attitude of the chaser. The magnetic force created by the chaser on the target depends on every state of the formation: attitude of the chaser which drives the orientation of the chaser dipole, attitude of the target which modifies both the orientation and position (because of the lever-arm) of the target dipole, and relative distance between the two satellites.

Let's assess $\frac{\partial\mathbf{F}_{C_{th}}}{\partial\boldsymbol{\theta}_C}$.

$$\mathbf{F}_{C_{th_O}} = \mathbf{P}_{B_C\to O}\mathbf{F}_{C_{th_B}} \tag{30}$$

which immediately yields:

$$\frac{\partial\mathbf{F}_{C_{th_O}}}{\partial\theta_{C_i}} = \frac{\partial\mathbf{P}_{B_C\to O}}{\partial\theta_{C_i}}\mathbf{F}_{C_{th_B}} \tag{31}$$

Let's assess $\frac{\mathbf{F}_{T_{\epsilon\mu}}}{\partial \mathbf{s}}$. Magnetic forces in the "far field" range are classically described by:

$$\mathbf{F}_{T_{\epsilon\mu}} = \frac{3\mu_0}{4\pi d^4}\left(\left(\boldsymbol{\mu}_C \cdot \hat{\mathbf{d}}\right)\boldsymbol{\mu}_T + \left(\boldsymbol{\mu}_T \cdot \hat{\mathbf{d}}\right)\boldsymbol{\mu}_C \right.$$
$$\left. + (\boldsymbol{\mu}_C \cdot \boldsymbol{\mu}_T)\,\hat{\mathbf{d}} - 5\left(\boldsymbol{\mu}_C \cdot \hat{\mathbf{d}}\right)\left(\boldsymbol{\mu}_T \cdot \hat{\mathbf{d}}\right)\hat{\mathbf{d}}\right) \quad (32)$$

This expression can be written

$$\mathbf{F}_{T_{\epsilon\mu}} = \frac{3\mu_0}{4\pi}\boldsymbol{\Psi}_T \boldsymbol{\mu}_C = \frac{3\mu_0}{4\pi}\boldsymbol{\Psi}_C \boldsymbol{\mu}_T \quad (33)$$

with $\boldsymbol{\Psi}_i$ depending on both the dipole i considered and $\mathbf{d} = \boldsymbol{\gamma}_{\mu_T} - \mathbf{s}$ the distance between the two dipoles:

$$\boldsymbol{\Psi}_i\left(\boldsymbol{\mu}_i, \mathbf{d}\right) = -\frac{5}{d^7}\left(\boldsymbol{\mu}_i \cdot \mathbf{d}\right)\begin{bmatrix} d_x^2 & d_x d_y & d_x d_z \\ d_x d_y & d_y^2 & d_y d_z \\ d_x d_z & d_y d_z & d_z^2 \end{bmatrix} + \frac{\left(\boldsymbol{\mu}_i \cdot \mathbf{d}\right)}{d^5}\mathbf{I}_3$$
$$+ \frac{1}{d^5}\begin{bmatrix} 2\mu_{i_x}d_x & \mu_{i_x}d_y + \mu_{i_y}d_x & \mu_{i_x}d_z + \mu_{i_z}d_x \\ \mu_{i_x}d_y + \mu_{i_y}d_x & 2\mu_{i_y}d_y & \mu_{i_y}d_z + \mu_{i_z}d_y \\ \mu_{i_x}d_z + \mu_{i_z}d_x & \mu_{i_y}d_z + \mu_{i_z}d_y & 2\mu_{i_z}d_z \end{bmatrix} \quad (34)$$

Therefore the differentiation of the magnetic force with regard to the relative position is:

$$\frac{\partial \mathbf{F}_{T_{\epsilon\mu}}}{\partial s_i} = -\frac{3\mu_0}{4\pi}\frac{\partial \boldsymbol{\Psi}_C}{\partial d_i}\boldsymbol{\mu}_T \quad (35)$$

Let's now differentiate $\mathbf{F}_{T_{\epsilon\mu}}$ with regard to the attitudes of both spacecraft, in the orbital frame.

$$\mathbf{F}_{T_{\epsilon\mu_O}} = \frac{3\mu_0}{4\pi}\boldsymbol{\Psi}_{T_O}\mathbf{P}_{B_C \to O}\boldsymbol{\mu}_{C_B} \quad (36)$$

yields:

$$\frac{\partial \mathbf{F}_{T_{\epsilon\mu_O}}}{\partial \theta_{C_i}} = \frac{3\mu_0}{4\pi}\boldsymbol{\Psi}_{T_O}\frac{\partial \mathbf{P}_{B_C \to O}}{\partial \theta_{C_i}}\boldsymbol{\mu}_{C_B} \quad (37)$$

As $\mathbf{d}$ depends on $\boldsymbol{\theta}_T$ via $\boldsymbol{\gamma}_{\mu_T}$ we have to compute:

$$\frac{\partial \mathbf{d}_O}{\partial \theta_{T_i}} = \frac{\partial \mathbf{P}_{B_T \to O}}{\partial \theta_{T_i}}\boldsymbol{\gamma}_{\mu_{T_B}} \quad (38)$$

then the differentiation $\frac{\partial \mathbf{F}_{T_{\epsilon\mu_O}}}{\partial \theta_{T_i}}$ is:

$$\frac{\partial \mathbf{F}_{T_{\epsilon\mu_O}}}{\partial \theta_{T_i}} = \frac{3\mu_0}{4\pi}\left(\sum_{j\in\{x,y,z\}}\frac{\partial \boldsymbol{\Psi}_{C_O}}{\partial d_{O_j}}\frac{\partial d_{O_j}}{\partial \theta_{T_i}}\right)\mathbf{P}_{B_T \to O}$$
$$+ \frac{3\mu_0}{4\pi}\boldsymbol{\Psi}_{C_O}\frac{\partial \mathbf{P}_{B_T \to O}}{\partial \theta_{T_i}}\boldsymbol{\mu}_{T_B} \quad (39)$$

5.2 Linearised Torques

Amongst the different torques applying to both satellites and given in (5), only the perturbation torque is supposed to be constant with regards to the different parameters. All the others depend on the relative position $\mathbf{s}$ and attitudes $\boldsymbol{\theta}_C$ and $\boldsymbol{\theta}_T$. In this section, they are linearised.

Torques on both satellites: gravity gradient and Earth magnetic

To begin, let's assess $\frac{\partial \boldsymbol{\tau}_{i_g}}{\partial \theta_i}$. The torque due to the gravity gradient is given for each satellite by:

$$\boldsymbol{\tau}_{g_B} = \frac{3\mu}{r^3}\hat{\mathbf{z}}_{O_B} \times \mathbf{J}\hat{\mathbf{z}}_{O_B} \quad (40)$$

which yields:

$$\frac{\partial \boldsymbol{\tau}_{g_B}}{\partial \theta_i} = \frac{3\mu}{r^3}\left(\left[\frac{\partial \mathbf{P}_{O \to B}}{\partial \theta_i}\begin{bmatrix}0\\0\\1\end{bmatrix}\right]^\times \mathbf{J}_B \mathbf{P}_{O \to B}\begin{bmatrix}0\\0\\1\end{bmatrix}\right.$$
$$\left. + \left[\mathbf{P}_{O \to B}\begin{bmatrix}0\\0\\1\end{bmatrix}\right]^\times \mathbf{J}_B\frac{\partial \mathbf{P}_{O \to B}}{\partial \theta_i}\begin{bmatrix}0\\0\\1\end{bmatrix}\right) \quad (41)$$

The magnetic torques depend on the three state parameters. The torque created by a magnetic field $\mathbf{B}_1$ on a dipole $\boldsymbol{\mu}_2$ is given by:

$$\boldsymbol{\tau}_{1/2} = \boldsymbol{\mu}_2 \times \mathbf{B}_1 \quad (42)$$

where in the "far-field" domain, the field $\mathbf{B}_1$ generated by the dipole $\boldsymbol{\mu}_1$ can be expressed by:

$$\mathbf{B}_1 = \frac{\mu_0}{4\pi d^3}\left(3\left(\boldsymbol{\mu}_1 \cdot \hat{\mathbf{d}}\right)\hat{\mathbf{d}} - \boldsymbol{\mu}_1\right) \quad (43)$$

This expression can also be written:

$$\mathbf{B}_1 = \frac{\mu_0}{4\pi}\boldsymbol{\Gamma}\boldsymbol{\mu}_1 \quad (44)$$

where $\boldsymbol{\Gamma}\left(\mathbf{d}\right)$ is the matrix defined by:

$$\boldsymbol{\Gamma}\left(\mathbf{d}\right) = \frac{3}{d^5}\begin{bmatrix} d_x^2 & d_x d_y & d_x d_z \\ d_x d_y & d_y^2 & d_y d_z \\ d_x d_z & d_y d_z & d_z^2 \end{bmatrix} - \frac{1}{d^3}\mathbf{I}_3 \quad (45)$$

For both satellites, the linearised magnetic torque due to the Earth is then given by:

$$\frac{\partial \boldsymbol{\tau}_{\epsilon\mu_{E_B}}}{\partial \theta_i} = \left[\boldsymbol{\mu}_B^\times\right]\frac{\partial \mathbf{P}_{O \to B}}{\partial \theta_i}\mathbf{B}_{E_O} \quad (46)$$

Torques on chaser: magnetic torque from the target
Similarly to (46), here is the magnetic torque on the chaser due to the target linearised with regard to the chaser's attitude:

$$\frac{\partial \boldsymbol{\tau}_{C_{\epsilon\mu_{B_C}}}}{\partial \theta_{C_i}} = \frac{\mu_0}{4\pi}\left[\boldsymbol{\mu}_{C_B}^\times\right]\frac{\partial \mathbf{P}_{O \to B_C}}{\partial \theta_{C_i}}\boldsymbol{\Gamma}_O\boldsymbol{\mu}_{T_O} \quad (47)$$

Because of the lever-arm $\boldsymbol{\gamma}_{\mu_T}$ existing between the CoM of the target and the position of its dipole, the expression of the magnetic torque on the chaser due to the target, linearised with regard to the target's attitude is quite different:

$$\frac{\partial \boldsymbol{\tau}_{C_{\epsilon\mu_{B_C}}}}{\partial \theta_{T_i}} = \frac{\mu_0}{4\pi}\left[\boldsymbol{\mu}_{C_B}^\times\right]\mathbf{P}_{O \to B_C}\left(\boldsymbol{\Gamma}_O\frac{\partial \mathbf{P}_{B_T \to O}}{\partial \theta_{T_i}}\boldsymbol{\mu}_{T_B}\right.$$
$$\left. + \sum_{j\in\{x,y,z\}}\left(\frac{\partial \boldsymbol{\Gamma}_O}{\partial d_{O_j}}\frac{\partial d_{O_j}}{\partial \theta_{T_i}}\right)\boldsymbol{\mu}_{T_O}\right) \quad (48)$$

The differentiation of this torque with regard to the relative position is given by:

$$\frac{\partial \boldsymbol{\tau}_{C_{\epsilon\mu_{B_C}}}}{\partial s_i} = -\frac{\mu_0}{4\pi}\left[\boldsymbol{\mu}_{C_B}^\times\right]\mathbf{P}_{O \to B_C}\frac{\partial \boldsymbol{\Gamma}_O}{\partial d_{O_j}}\boldsymbol{\mu}_{T_O} \quad (49)$$

Torques on target: magnetic torque from the chaser
Here is the expression of the magnetic torque on the target due to the chaser, linearised with regard to the target's attitude:

$$\frac{\partial \boldsymbol{\tau}_{T_{\epsilon\mu_{B_T}}}}{\partial \theta_{T_i}} = \frac{\mu_0}{4\pi}\left[\boldsymbol{\mu}_{T_B}^\times\right]\left(\frac{\partial \mathbf{P}_{O \to B_T}}{\partial \theta_{T_i}}\boldsymbol{\Gamma}_O\boldsymbol{\mu}_{C_O}\right.$$
$$\left. + \mathbf{P}_{O \to B_T}\sum_{j\in\{x,y,z\}}\left(\frac{\partial \boldsymbol{\Gamma}_O}{\partial d_{O_j}}\frac{\partial d_{O_j}}{\partial \theta_{T_i}}\right)\boldsymbol{\mu}_{C_O}\right) \quad (50)$$

Again because of the lever-arm $\boldsymbol{\gamma}_{\mu_T}$, the expressions of the linearised magnetic torque due to the other satellite differ between both spacecraft. Here is given $\frac{\partial \boldsymbol{\tau}_{\epsilon\mu_{C/T_{B_T}}}}{\partial \theta_{C_i}}$:

$$\frac{\partial \boldsymbol{\tau}_{T_{\epsilon\mu_{B_T}}}}{\partial \theta_{C_i}} = \frac{\mu_0}{4\pi}\left[\boldsymbol{\mu}_{T_B}^\times\right]\mathbf{P}_{O\to B_T}\boldsymbol{\Gamma}_O\frac{\partial \mathbf{P}_{B_C\to O}}{\partial \theta_{C_i}}\boldsymbol{\mu}_{C_{B_C}} \quad (51)$$

The differentiation of this torque with regard to the relative position is given by:

$$\frac{\partial \boldsymbol{\tau}_{T_{\epsilon\mu_{B_T}}}}{\partial s_i} = -\frac{\mu_0}{4\pi}\left[\boldsymbol{\mu}_{T_B}^\times\right]\mathbf{P}_{O\to B_T}\frac{\partial \boldsymbol{\Gamma}_O}{\partial d_{O_j}}\boldsymbol{\mu}_{C_O} \quad (52)$$

Torques on target: lever-arm torque from the chaser
The differentiation of the torque due to the lever-arm, with regard to the attitude of the target is given by:

$$\frac{\partial \boldsymbol{\tau}_{T_{\gamma_{B_T}}}}{\partial \theta_{T_i}} = \frac{3\mu_0}{4\pi}\left[\boldsymbol{\gamma}_{\mu_T}^\times\right]\left(\frac{\partial \mathbf{P}_{O\to B_T}}{\partial \theta_{T_i}}\boldsymbol{\Psi}_{CO}\boldsymbol{\mu}_{T_O}\right.$$
$$+\mathbf{P}_{O\to B_T}\sum_{j\in\{x,y,z\}}\left(\frac{\partial \boldsymbol{\Psi}_{CO}}{\partial d_{O_j}}\frac{\partial d_{O_j}}{\partial \theta_{T_i}}\right)\boldsymbol{\mu}_{T_O} \quad (53)$$
$$\left.+\mathbf{P}_{O\to B_T}\boldsymbol{\Psi}_{CO}\frac{\partial \mathbf{P}_{B_T\to O}}{\partial \theta_{T_i}}\boldsymbol{\mu}_{T_B}\right)$$

The linearisation of this torque with regards to the chaser attitude is given by:

$$\frac{\partial \boldsymbol{\tau}_{T_{\gamma_{B_T}}}}{\partial \theta_{C_i}} = \frac{3\mu_0}{4\pi}\left[\boldsymbol{\gamma}_{\mu_T}^\times\right]\mathbf{P}_{O\to B_T}\boldsymbol{\Psi}_{TO}\frac{\partial \mathbf{P}_{B_C\to O}}{\partial \theta_{C_i}}\boldsymbol{\mu}_{C_{B_C}} \quad (54)$$

And the linearisation with regards to the relative position is:

$$\frac{\partial \boldsymbol{\tau}_{T_{\gamma_{B_T}}}}{\partial s_i} = -\frac{3\mu_0}{4\pi}\left[\boldsymbol{\gamma}_{\mu_T}^\times\right]\frac{\partial \boldsymbol{\Psi}_C}{\partial d_{O_i}}\boldsymbol{\mu}_T \quad (55)$$

6. CONTROL OF THE FORMATION AROUND NOMINAL

The previous sections have derived a linearised model of the dynamics around a given trajectory briefly described in section 3.3. This linear model is time dependent, because the nominal states are not constant in time: their variations are due to the variations of $\mathbf{B}_{E_O}$, r, $\boldsymbol{\omega}$ and $\boldsymbol{\eta}$ in orbit, and to the different inertias making the guidance problem a differential problem. This is not much developed in this paper for lack of space, but will be explained in a paper to be published by the same authors.

The aim of this section is to evaluate the linearisation previously derived, as well as to get a first glance on the behaviour of the closed loop system with two possible controllers. To do so properly, we should directly compare the full non-linear model with the Linear Time Varying (LTV) model derived in the previous sections. However, in the frame of this preliminary study, we will assume in the following that the evolution of $\mathbf{B}_{E_O}$, r, $\boldsymbol{\omega}$ and $\boldsymbol{\eta}$ are slow enough for the nominal state to be considered constant during the simulation. Then $\mathbf{G}(t)$ can be approximated by $\mathbf{G}(t_0)$, and the non-linear system compared to the Linear Time Invariant (LTI) plant $\mathbf{G}(t_0)$.

The nominal parameters used are:
$\mathbf{s} = [8.15\ 0.70\ 0.22]^T$ m; $\boldsymbol{\theta}_T = [3\ \text{-}18\ 149]^T$ deg; $\boldsymbol{\theta}_C = [0\ 0\ 0]^T$ deg; $\boldsymbol{\mu}_{C_O} = [\text{-}2.29\ \text{-}8.17\ \text{-}2.33]^T \times 10^5$ Am^2; $\mathbf{F}_{C_{th_O}} = [50\ 0\ 0]^T$ mN.
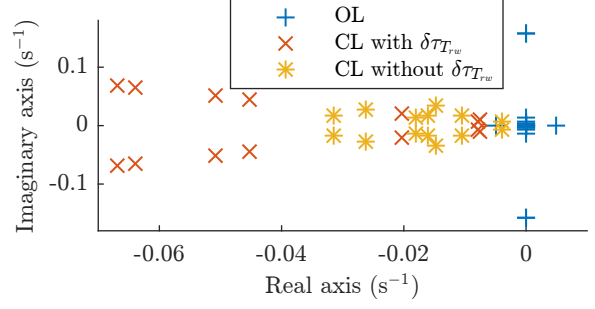

Fig. 2. Poles of open and closed loops (zoom on the origin)

The poles of the open loop system are presented in Fig. 2, and highlight its instability. To control the formation, two cases are considered and developed hereafter.

6.1 Control with $\boldsymbol{\delta\tau}_{T_{rw}}$

In the first case, the attitude of the target is assumed controlled by its AOCS through $\boldsymbol{\delta\tau}_{T_{rw}}$ in a decentralised controller:

$$\boldsymbol{\delta\tau}_{T_{rw}} = \mathbf{K}_1\left[\boldsymbol{\delta\theta}_T\ \boldsymbol{\delta\omega}_T\right]^T \quad (56)$$

In this case, simulations have showed that there is no need for the chaser to use $\boldsymbol{\delta F}_{C_{th}}$. The rest of the inputs are controlled by a centralised controller on the chaser:

$$\left[\boldsymbol{\delta\tau}_{C_{rw}}\ \boldsymbol{\delta\mu}_C\right]^T = \mathbf{K}_2\left[\boldsymbol{\delta s}\ \boldsymbol{\dot{\delta}s}\ \boldsymbol{\delta\theta}_C\ \boldsymbol{\delta\omega}_C\right]^T \quad (57)$$

The two state feedback controllers $\mathbf{K}_1$ and $\mathbf{K}_2$ are designed using LQ synthesis with minimum energy tuning of the two submodels of $\mathbf{G}$ (see (27)): $\mathbf{G}_{13:18,10:12}$ and
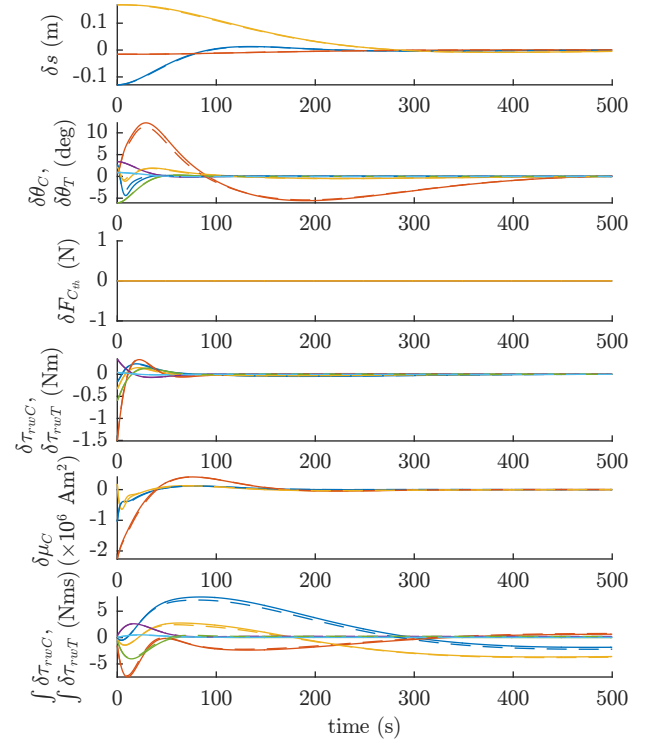

Fig. 3. Evolution of states and control inputs, for control with $\boldsymbol{\delta\tau}_{T_{rw}}$. Linear model in plain, non-linear in dashed line. Chaser in blue-red-yellow, target in purple-green-cyan when applicable.

$\mathbf{G}_{1:12,1:9}$ respectively, where $\mathbf{G}_{i:j,k:l}$ stands for the minimal realisation of the subsystems of $\mathbf{G}$ between inputs k to l and outputs i to j. Thus, the design ignores dynamic couplings between the two subsystems, but they are taken into account in the simulations presented in Fig. 3. The poles of the closed loop are presented in Fig. 2.

As it can be seen in Fig. 3, the linear model (in plain lines) behaves similarly to the non-linear model (in dashed lines). The behaviour of the system is acceptable when confronted to an initial perturbation, as long as this perturbation does not exceed the limits of the linearisation, which seem tighter on the attitudes. This is consistent with results foun by Ahsun et al. (2010). The magnetic dipole needed is consistent with the values given by Schweighart (2005) and Elias et al. (2007). The torque and angular momentum storage capacity needed for both satellites lie within the capacity of devices like the *CMG 15-45S* by Airbus DS.

6.2 Control without $\boldsymbol{\delta\tau}_{T_{rw}}$

In the second case considered, the target is not assumed to control its attitude. The controller $\mathbf{K}_3$ is designed in the same way that $\mathbf{K}_1$ and $\mathbf{K}_2$: an LQ synthesis on $\mathbf{G}_{1:18,1:9}$, but uses a full state feedback and all controls but $\boldsymbol{\delta\tau}_{T_{rw}}$:

$$[\boldsymbol{\delta}\mathbf{F}_{C_{th}}\ \boldsymbol{\delta\tau}_{C_{rw}}\ \boldsymbol{\delta\mu}_C]^T = \mathbf{K}_3 \left[\boldsymbol{\delta}\mathbf{s}\ \dot{\boldsymbol{\delta}}\mathbf{s}\ \boldsymbol{\delta\theta}_C\ \boldsymbol{\delta\omega}_C\ \boldsymbol{\delta\theta}_T\ \boldsymbol{\delta\omega}_T\right]^T \tag{58}$$

In this case, as it can be seen in Fig. 2, the slowest poles of the closed loop are still located approximately at the same frequency and damping as in the previous control scheme. However, more of them are located at the same low frequency, which causes a slower convergence of this system, as shown in Fig. 4, where the simulation is run with the same initial conditions as in Fig. 3. Moreover, to control the system without using $\boldsymbol{\delta\tau}_{T_{rw}}$, higher values are needed for $\boldsymbol{\delta}\mathbf{F}_{C_{th}}$, of the order of $1\,\mathrm{N}$. In addition, although the torque needed stays acceptable (of the order $0.5\,\mathrm{N\,m}$), the angular momentum storage of the chaser must be increased approximately by a factor 10. To finish, this controller shows reduced margins when tested with the non-linear model. The Linear Time Varying behaviour is currently under investigations.

7. CONCLUSION AND FUTURE WORK

Magnetic tugging is a new concept, which dynamics, guidance and control are complex. In this paper, we have developed and linearised the non-linear equations describing the evolution of such a 2-satellites electromagnetic formation. This linearisation has been showed accurate, hence validating the linear model.

Two controllers have been shown. The first one is adapted to a configuration where the target is able to control its own attitude via its AOCS. This controller shows satisfying results. In the case where the attitude of the target has to be controlled by the chaser, the behaviour of the system is still acceptable, but margins are reduced and requirements on the actuators increased.

For this early study, the non-linear time varying system has been approximated by an LTI plant. This gives a first hint on the efficiency of the controllers proposed, although
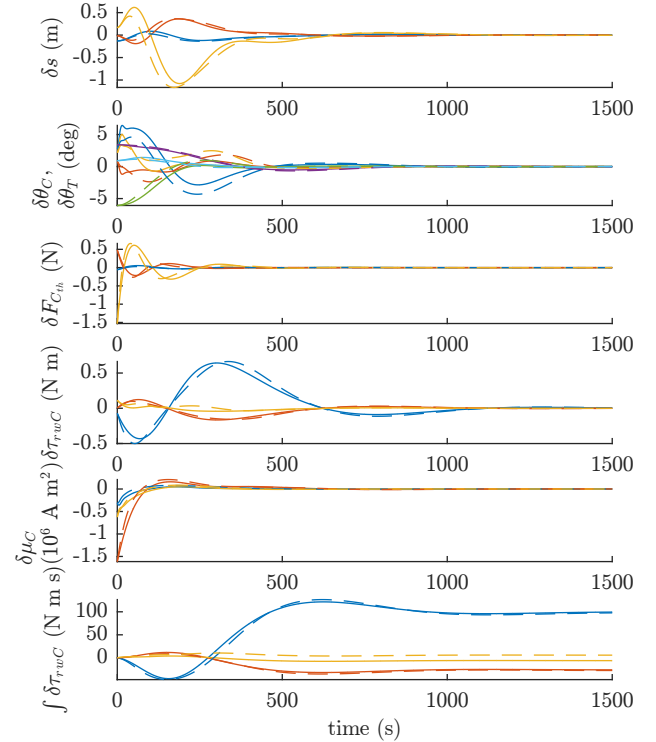

Fig. 4. Evolution of states and control inputs, for control without $\boldsymbol{\delta\tau}_{T_{rw}}$. Same lines/colors as Fig. 3.

it does not suffice to claim satisfying results for the time-varying plant. To address this problem, LTV controllers will have to be designed and tested on the non-linear time-varying system.

REFERENCES

Ahsun, U. and Miller, D.W. and Ramirez-Riberos, J.L. Control of electromagnetic satellite formations in near-earth orbits, J. Guid. Control Dyn. (2010)

Elias, L.M. and Kwon, D.W. and Sedwick, R.J. and Miller, D.W. Electromagnetic formation fight dynamics including reaction wheel gyroscopic stiffening effects, Journal of Guidance Control and Dynamics (2007)

Fabacher, E., Lizy-Destrez, S., Alazard, D., Ankersen, F., and Jourdas, J.F. Guidance and navigation for electro-magnetic formation flight orbit modification. EuroGNC, Toulouse (2015)

Sakai, S. and Kaneda, R. and Maeda, K. and Saitoh, T. and Saito, H. and Hashimoto, T. Electromagnetic formation flight for LEO satellites, 17th Workshop on JAXA Astrodynamics and Flight Mechanics (2008)

Voirin, T and Kowaltschek, S. and Dubois-Matra, O. NOMAD: a contactless technique for active large debris removal, IAC, Naples (2008)

Huang, X. and Zhang, C. and Ban, X. Dipole solution and angular-momentum minimization for two-satellite electromagnetic formation flight, Acta Astronautica (2016)

Schweighart, S.A. Electromagnetic formation flight dipole solution planning. PhD Thesis, MIT (2005)

Wie, B. Space Vehicle Dynamics and Control, AIAA, (1998)